Higher-order Mode Rectangular Dielectric Resonator Antenna for 5G Applications

Nor Hidayu Shahadan[1], Muhammad Ramlee Kamarudin*[2], Mohd Haizal Jamaluddin[3], Yoshihide Yamada[4]
[1]Department of Polytechnic, Ministry of Education Malaysia, Presint 4, 62100 W.P. Putrajaya, Malaysia
[1,2,3]Wireless Communication Centre (WCC), Universiti Teknologi Malaysia, UTM Johor,
Johor 81310, Malaysia
[4]Malaysia-Japan International Institute of Technology (MJIIT), Universiti Teknologi Malaysia,
54100 K. L., Malaysia
*Corresponding author, e-mail: ramlee@fke.utm.my

Abstract

The excitation of the higher-order mode, $TE^y{}_{1\delta 3}$ in rectangular dielectric resonator designed was explored to enhance the antenna gain and detailed elaboration is presented in this paper. The antenna was fed by a 50Ω microstrip line through an aperture cut in the ground plane. Besides avoiding spurious radiation, this feeding technique gives flexibility in controlling the amount of coupling in order to reduce the Q-factor in the higher-order mode RDRA. A design was developed and subsequently simulated using Ansoft HFSS ver 16.0 by utilizing Duroid 5880 dielectric substrate with a thickness (ts) of 0.254 mm, a permittivity (εs) of 2.2 and a loss tangent (δ) of 0.001 at 15 GHz. The higher-order mode, $TE^y{}_{1\delta 3}$ RDRA achieved the measured gain at 9.76 dBi and the measured impedance bandwidth as much 2.5 GHz which is 4.7% more compared to the fundamental mode, $TE^y{}_{1\delta 1}$. The result should be considered suitable for 5G applications.

Keywords: higher-order mode, dielectric resonator antenna, bandwidth, gain, 5G

1. Introduction

Advancement in telecommunication technology has evolved into 5G (5th Generation). Due to a shortage of frequency spectrum below 6 GHz, the millimeter-wave (10-100 GHz) was considered as a potential carrier frequency for the 5G technology [1]. However, based on Friss formula, the free space loss is much more at the higher frequency because of shorter wavelength. Consequently, the antenna gain needs to be increased to compensate the anticipated incremental loss. An alternative method to fulfill the 5G technology is to increase the bandwidth of the antenna to meet the requirements for long distance communication [2].

Recent studies on dielectric resonator antennas (DRA) have indicated that DRAs have some intriguing advantages such as wider bandwidth and lower loss compared to a microstrip patch antenna thus it is more suitable for higher frequencies applications [3]. Rectangular shapes are frequently chosen because of simpler fabrication and better degrees of freedom in comparison to other common shapes such as hemispherical or cylindrical. In addition, rectangular DRAs are normally excited in the fundamental mode, $TE^x{}_{\delta 11}$ or $TE^y{}_{1\delta 1}$ with an ordinary gain of about 5 dBi, when employed on a large ground plane [4].

Several approaches are suggested to increase the gain of the DRAs. An array of single-element combined using a feed network [5] is probably the most versatile method in which the gain value is directly influenced by the number of elements. Besides, stacking DRAs on top of each other [6], creating a shallow pyramidal horn [7], positioning a circularly polarized DRA within a circular cavity [8] and the deployed dielectric superstrates as additional structures [9] are proven as being able to increase the gain of a DRA. In some of these cases, it can also improve the impedance bandwidth of the antenna. Nevertheless, most of these methods need a significant increase in surface area, complexity and costs.

Altering the single element DRA by utilizing higher-order radiation modes is another technique to increase the gain. This method has already been used in both cylindrical and rectangular DRAs. Research in [10] stated that the rectangular dielectric resonator antenna

(RDRA) excited on higher-order $TE_{\delta 13}$ and $TE_{\delta 15}$ modes can attain the gain of 8.2 dBi and 10.2 dBi, respectively. However, the impedance bandwidth decreases as the height of the rectangular dielectric resonator (RDR) is increased. This is due to the larger ratio of volume (*V*) to surface (*S*) in the $TE_{\delta 15}$ mode compared to the $TE_{\delta 13}$ mode that also increased the *Q*-factor. The impedance bandwidth of the antenna can be expanded by reducing the *Q*-factor through control of coupling amount from the feed to the resonator. Up till now, based on the authors' knowledge, no such study has been carried out to address the effect of the coupling mechanism to determine the enhancement in bandwidth as well as achievable gain through excitation in the higher-order mode.

In this study, an excitation at the higher-order mode, $TE^{y}_{1\delta 3}$ was used in a single RDR to achieve sufficient gain enhancement. The RDR was mounted on the ground plane with slot aperture and fed using a microstrip line. A parametric study using Ansoft High Frequency Structural Simulator (HFSS) ver 16.0 was conducted in Section 2 for several combination values of the RDR heights (*h*), the slot width (*Ws*), the stub lengths (*S*), and the microstrip line widths (*W*) to observe various effects to the gain and impedance bandwidth in the $TE^{y}_{1\delta 3}$ mode. The determining factors of the coupling amount according to the optimized parameter values that reduced the *Q*-factor and increased the bandwidth of the antenna even in the higher-order mode are also presented in this section. In Section 3, the fabricated RDRA and the results based on observations are discussed. Finally, the summary of this study is concluded in Section 4.

2. Antenna Design, Analysis and Optomization

In this paper, the RDRA is positioned on the ground plane side of a dielectric substrate and fed by a 50Ω microstrip line through an aperture cut in the ground plane. The aperture coupled design is chosen because its feed network can isolate the antenna from the ground plane and thus avoid spurious radiation from the feed. The following equations are used to design the rectangular slot in the ground plane. The slot length,

$$L_s = \frac{0.4\lambda_o}{\sqrt{\varepsilon_e}} \tag{1}$$

Where λ_o is the wavelength and the effective permittivity is defined as:

$$\varepsilon_e = \frac{\varepsilon_r + \varepsilon_s}{2} \tag{2}$$

Where ε_r and ε_s are the dielectric constant of the RDR and substrate, respectively. The slot width,

$$W_s = 0.2 L_s \tag{3}$$

And the stub length,

$$S = \frac{\lambda_g}{4} \tag{4}$$

Where λ_g is the guided wave in the substrate.

The resonant frequencies, f_o of the $TE^{y}_{m\delta n}$ with a dielectric constant, ε_r can be predicted using Equation (5) derived from the dielectric waveguide model [4]. The following equations are obtained for the wavenumber k_x, k_y and k_z where m and n are index numbers.

$$k_x = \frac{m\pi}{d}, \ k_y \tan\left(\frac{k_y w}{2}\right) = \sqrt{(\varepsilon_r - 1)k^2{}_0 - k^2{}_y} \text{ and } k_z = \frac{n\pi}{2h} \tag{5}$$

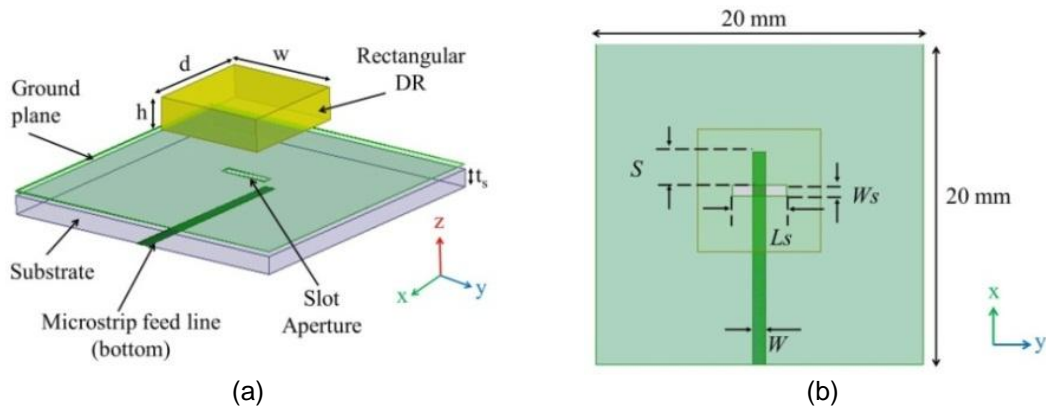Where k_0 denotes the free-space wavenumber corresponding to the resonant frequency.

Figure 1. Configuration of the RDRA excited in the fundamental mode, $TE^y_{1\delta1}$ (a) 3D view
(b) Top view

First, for the RDRA excited in the fundamental mode ($TE^y_{1\delta1}$), it was designed to resonate at 15 GHz, with a dielectric constant of $\varepsilon_r = 10$ and dimensions of $w = d = 7.5$ mm and $h = 1.8$ mm. The design values are implemented and then simulated using Ansoft High Frequency Structural Simulator (HFSS) ver 16.0 to obtain optimum parameter values. Duroid 5880 dielectric substrate with a thickness (t_s) of 0.254 mm, a permittivity (ε_s) of 2.2 and a loss tangent (δ) of 0.001 is used in the design. For this case, all parameter values involved in the aperture coupled feed satisfactorily fulfilled all the Equations (1) - (4). The configuration of the RDRA excited in the $TE^y_{1\delta1}$ mode is as shown in Figure 1.

Next, the RDRA excited in the higher-order mode ($TE^y_{1\delta3}$) as depicted in Figure 2 was applied at 15 GHz with increased antenna dimension in normal to ground plane directions and offered higher gain until dipole overlapping had disappeared. Hence, the theory of short magnetic dipoles defined that the modes in the minimum spacing (s), between the short magnetic dipoles should be equal to 0.4λ [10]. To establish the concept of this study, observations were made by varying the height of RDR as shown in Figure 3. Apparently, it indicates that the gain increases as the height of RDR is increased. However, it was observed that the gain started to decrease, even in the higher-order mode, the moment magnetic dipole began to overlap. Figure 4 shows the simulated H_y field inside the RDR and the $TE^y_{1\delta3}$ mode is approximately spaced, $s = 9.2$ mm apart which corresponds to 0.46λ. The optimized higher-order mode RDR dimensions are given as: $w = d = 4$ mm and $h = 11.5$ mm.
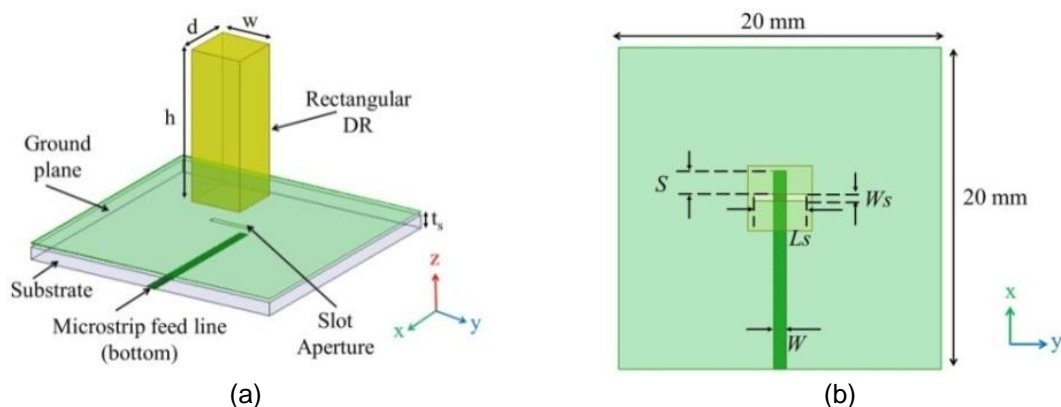

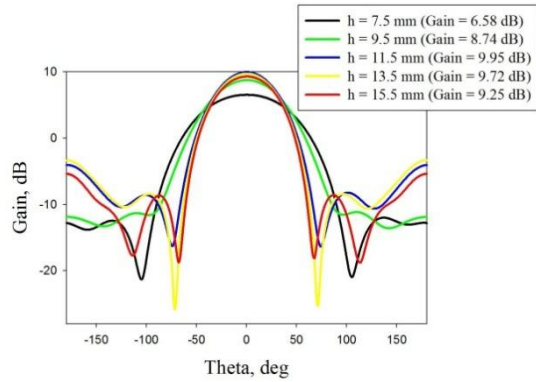Figure 2. Configuration of the RDRA excited in the higher-order mode, $TE^y_{1\delta3}$ (a) 3D view
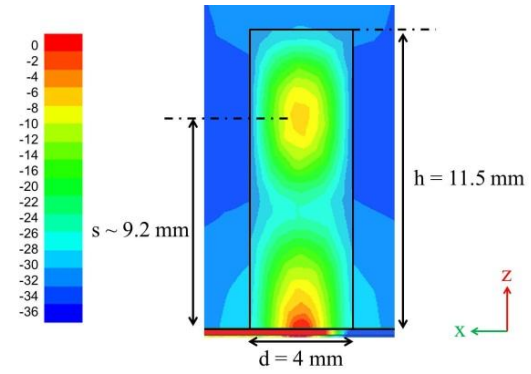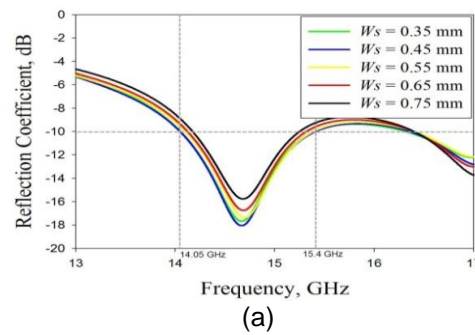(b) Top view
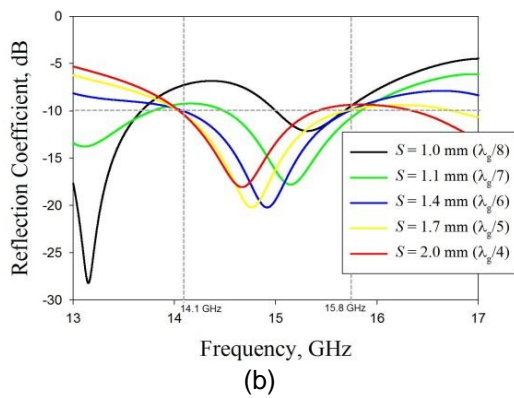
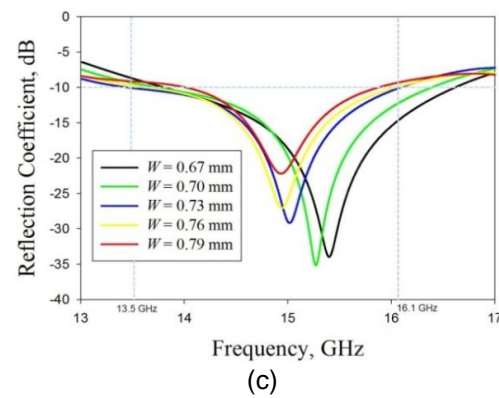Figure 3. Gain at various height of the RDR

Figure 4. H_y field in $TE^y_{1\delta3}$ mode

(a)

(b)

(c)

Figure 5. Characteristics of the impedance bandwidth performance of the RDRA excited in the $TE^y_{1\delta3}$ mode with (a) different slot width, *Ws* (b) different stub lengths, *S* (c) different microstrip line widths, *W*

A parametric study of the coupling mechanism involving the slot width (*Ws*), stub length (*S*) and the microstrip line width (*W*) was carried out to obtain the optimal impedance bandwidth. This study is important to ascertain the best dimension that provides the strongest electromagnetic coupling from the feed network to the RDR. Figure 5(a) shows the simulated reflection coefficients of the $TE^y_{1\delta3}$ mode by varying the slot widths, *Ws* from 0.35 mm to 0.75 mm. The impedance bandwidth was improved by 1 % at minimum reflection coefficients with reducing the *Ws* from 0.75 mm to 0.45 mm. Afterwards, the length of the stub, *S* was varied from 1 mm (λ_g/8) to 2 mm (λ_g/4) as shown in Figure 5(b). It is clearly indicated that the optimum impedance bandwidth with strong electromagnetic coupling between the dielectric resonator and the microstrip feed line can be achieved when the *S* is 1.4 mm, which was obtained through

extensive simulations resulted in minimum reflection coefficient and wider bandwidth. By reducing the S from $\lambda_g/4$ to $\lambda_g/6$, the impedance bandwidth was increased by 2%. In reference to the results described in Figure 5(c), it was observed that as the impedance bandwidth gets wider, the accomplished results are such that at W= 0.73 mm, it was 6% more as compared to W = 0.79 mm that was used in the design of the $TE^y_{1\delta1}$ mode. This study has proved that the parameters Ws (width of the slot), S (length of the stub) and W (width of the microstrip line) are the most critical influencing factors that impact the structure's adaptation. In order to have a good impedance matching at 15 GHz, the optimized parameters for the two structures are fixed as described in Table 1.

Table 1. Summary of the optimized parameters

Parameter (mm) Resonant Mode	w	d	h	Ls	Ws	S	W
Fundamental mode, $TE^y_{1\delta1}$	7.5	7.5	1.8	3.34	0.65	2	0.79
Higher-order mode, $TE^y_{1\delta3}$	4	4	11.5	3.34	0.4	1.4	0.73

The Q-factor of the antenna is the crucial parameter, which influences the bandwidth of the antenna. It is directly related to the unloaded Q of the resonant mode excited in the dielectric resonator. The unloaded Q-factor can be related to the geometrical characteristics of the resonator by the following equation:

$$Q = 2\omega_o \frac{Stored\ Energy, W_e}{Radiated\ power, P_{rad}} \propto 2\omega_o \varepsilon_r^p \left(\frac{Volume}{Surface}\right)^s \tag{6}$$

With $p > s \geq 1$, where ω_o is the resonant angular frequency and ε_r is the relative dielectric constant. Equation (6) indicated that the Q-factor is reduced if the volume (V) to surface (S) ratio is minimized, thus increased the bandwidth of the antenna. Table 2 compares the dimensions of the RDRs operating in the $TE^y_{1\delta1}$ mode and the $TE^y_{1\delta3}$ mode. In reference to the table, the (V/S) ratio for the DRA excited in the $TE^y_{1\delta3}$ mode is higher than the $TE^y_{1\delta1}$ mode. It seems that the RDRA excited in the $TE^y_{1\delta1}$ mode resulted in wider bandwidth compared to the $TE^y_{1\delta3}$ mode. However, this equation failed to predict anything because it was assumed the RDRA was in isolation or mounted on an infinite perfect conducting ground plane and was not taking the coupling mechanism into account which is used to excite the RDR.

Table 2. Comparison of the volume to surface ratio between the RDR excited in the $TE^y_{1\delta1}$ and $TE^y_{1\delta3}$

Resonant mode	Dimensions $w \times d \times h\ (mm)$	Surface area $2[wd + dh + wh]\ (mm^2)$	Volume $wdh\ (mm^3)$	$\left(\frac{Volume, V}{Surface, S}\right)$
Fundamental mode, $TE^y_{1\delta1}$	7.5 × 7.5 × 1.8	166.5	101.3	0.61
Higher-order mode, $TE^y_{1\delta3}$	4.0 × 4.0 × 11.5	216	184	0.85

When coupling to RDRA, the amount of aperture coupling, χ between the source and the fields within the RDRA can be dictated by using the reciprocity theorem [5] with the appropriate boundary conditions. The coupling aperture can be equivalently modeled as two magnetic currents $(\vec{M^s})$ on the DR side and $-(\vec{M^s})$ on the feed side, respectively [11]. The amount of coupling:

$$\chi \propto \int_v (H_{DRA} \cdot M_s)dV \tag{7}$$

Where V is the volume filled by the source within the magnetic currents exist, while H_{DRA} is the magnetic fields within the DRA. Besides power transfer, the coupling mechanism at the RDRA has a loading effect that can influence the Q-factor of the RDRA. The loaded Q-factor of the RDRA is derived as follows:

$$Q_L = \frac{Q}{1+\chi} \tag{8}$$

Where Q is the unloaded Q-factor.
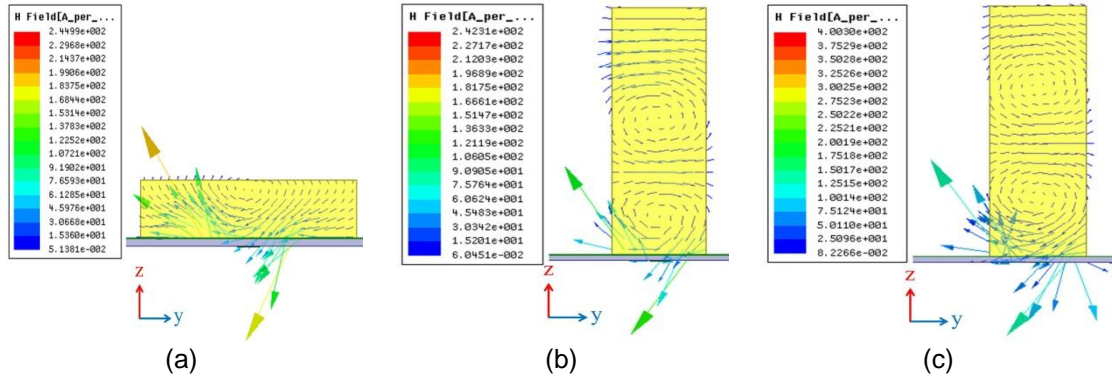

(a)   (b)   (c)

Figure 6. Magnetic field for the RDRA excited in the (a) $TE^y{}_{1\delta1}$ mode, (b) $TE^y{}_{1\delta3}$ mode before optimization (c) $TE^y{}_{1\delta3}$ mode after optimization

By optimizing the parameter values for the coupling mechanism RDRA excited in the $TE^y{}_{1\delta3}$ mode, the total magnetic field of the antenna was successfully increased. Figure 6(c) shows that RDRA excited in $TE^y{}_{1\delta3}$ mode has a stronger total magnetic field. From Equation (7), it was deduced that the amount of coupling, χ increases when the total magnetic field is increased. In verifying the accuracy of this analysis, the anticipated unloaded Q-factor was determined by calculating the stored electric energy (W_e) inside the resonator and the simulated radiated power (P_r).

$$W_e = \frac{2\varepsilon_0\varepsilon_r whd}{32}\left(1 + \frac{sin(2k_y h)}{2k_y h}\right)k_x^2 + k_z^2 \tag{9}$$

Table 3 shows the calculated loaded Q-factor from the normalized total H-field and the calculated and simulated bandwidth values based on several widths 'W' with a constant $S = \lambda_g/6$. Some errors exist in the bandwidth ranging from 5 to 11% that possibly due to the Q-factor in the transmission line causing such conductor loss and dielectric loss which were excluded in the calculated bandwidth values. Figure 7 and 8 depict the significant impact on the total Q-factor and bandwidth of the antenna due to the coupling mechanism. It was observed that by reducing the width of microstrip line (W), it increased the total H-field. Because of that, it reduced the loaded Q-factor in Equation (8), thus increased the bandwidth of the antenna.

Table 3. Comparison of the bandwidth between calculation and simulation for various widths of the microstrip line, W of the RDRA excited in the $TE^y{}_{1\delta3}$ mode

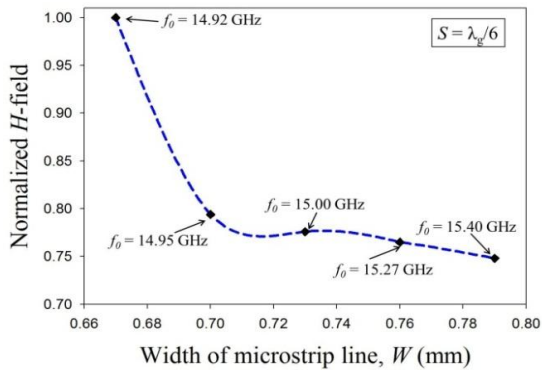| Width of the microstrip line, W (mm) with $S=\lambda_g/6$	0.67	0.70	0.73	0.76	0.79
Loaded Q-factor, Q_L (calculated)	2.74	3.05	3.08	3.10	3.13
Bandwidth, $BW = \frac{VSWR-1}{\sqrt{VSWR}\,Q_L}$ % (calculated)	25.80	23.18	22.96	22.81	22.59
Bandwidth, BW % (simulated)	18.22	17.69	17.55	16.01	11.4

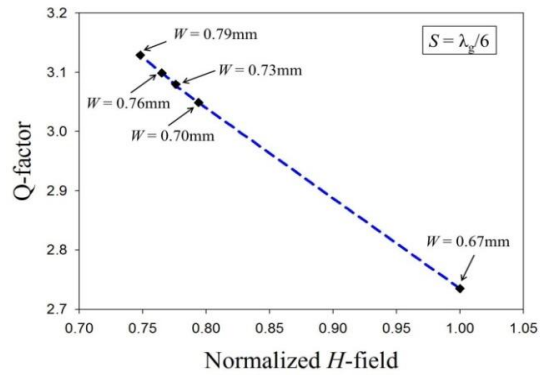Figure 7. Normalized total *H*-field for various widths of the microstrip line, *W*

Figure 8. Loaded *Q*-factor influenced by coupling mechanism

3. Results and Discussion

Based on the dimensions given in Table 1, both antennas were fabricated to validate the analyses that have been presented in the previous section. Photographs of the fabricated antennas are as illustrated in Figure 9. The antennas were measured and the results are consistent with the simulated results.
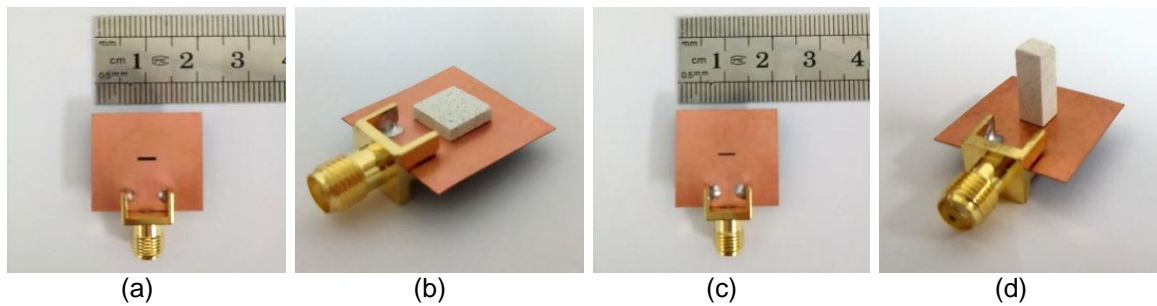

| (a) | (b) | (c) | (d) |

Figure 9: Photograph of the fabricated RDRA (a) Top view without RDR in the $TE^y_{1\delta1}$ mode (b) 3D view with RDR in the $TE^y_{1\delta1}$ mode (c) Top view without RDR in the $TE^y_{1\delta3}$ mode (d) 3D view with RDR in the $TE^y_{1\delta3}$ mode

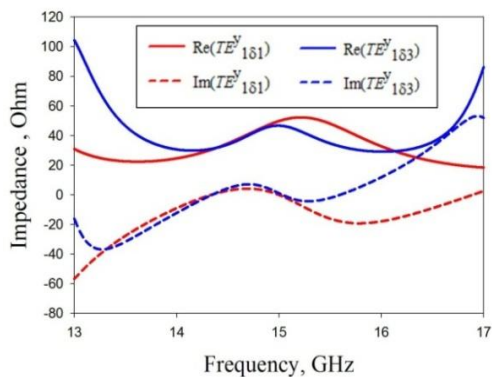### 3.1. Impedance Bandwidth and *Q*-factor
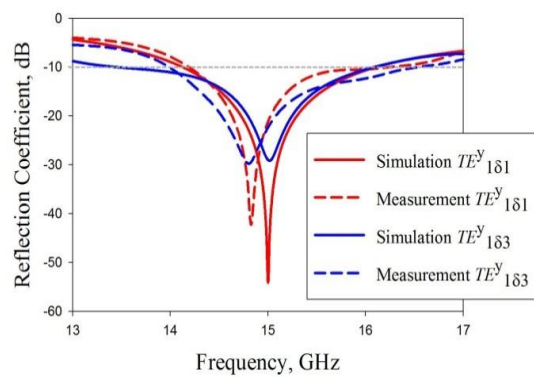

Figure 10. Comparison of the impedance matching

Figure 11. Comparison of the reflection coefficients

Figure 10 shows the simulated impedance curve of the RDRA excited in the $TE^y_{1\delta1}$ mode and the $TE^y_{1\delta3}$ mode. It can be observed that both antennas have a good impedance matching at 15 GHz. However, the measured $|S_{11}|$ depicted that there is a slight shift in the resonant frequency as shown in Figure 11 due to the fabrication tolerance of the DR. In reference to the figures, both designs have a good $|S_{11}|$ at 15 GHz. The measured 10-dB impedance bandwidth has achieved 2.5 GHz (17.2%) for DRA excited in the $TE^y_{1\delta3}$ mode but only 1.8 GHz (12.2%) was observed for RDRA excited in $TE^y_{1\delta1}$ mode.

3.2. Radiation Characteristics and Gain

The simulated and measured radiation pattern for *E*-plane and *H*-plane are compared as illustrated in Figure 12. As shown, both designs have a broadside radiation. Nevertheless, a narrower beamwidth result was achieved by RDRA excited in $TE^y_{1\delta3}$ mode, in comparison with the DRA excited in $TE^y_{1\delta1}$ mode. A spacing of *s* = 0.46λ, produces a good compromise between the beamwidth and sidelobe levels. Besides that, the measured gain for the RDRA excited in $TE^y_{1\delta3}$ mode has achieved 9.76 dBi in comparison to 5.04 dBi when excited in $TE^y_{1\delta1}$ mode as tabulated in Table 4. In short, by increasing the mode of the DR to $TE^y_{1\delta3}$, the gain of the antenna become almost 2 times higher than the $TE^y_{1\delta1}$.
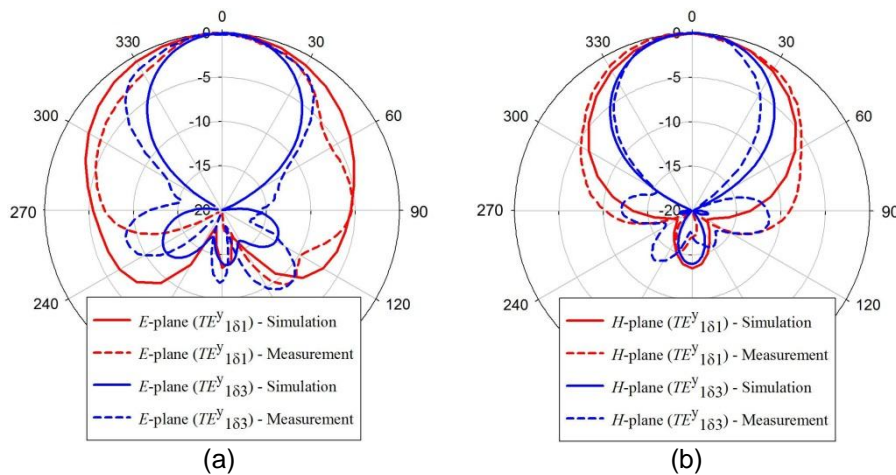

Figure 12. Comparison of the radiation patterns (a) *E*-plane (b) *H*-plane

Table 4. Comparison of the antenna gain

Gain of the single DRA	Simulated	Measured
Fundamental mode, $TE^y_{1\delta1}$	5.60 dBi	5.04 dBi
Higher-order mode, $TE^y_{1\delta3}$	9.95 dBi	9.76 dBi

4. Conclusion

A higher-order mode Rectangular Dielectric Resonator Antenna (RDRA) at 15 GHz was proposed and observations were made. The amount of coupling was altered to reduce the *Q*-factor. Coupling mechanism cause significant impact to the impedance bandwidth such that it achieved 2.5 GHz for RDRA excited in the $TE^y_{1\delta3}$ mode compared to 1.8 GHz for RDRA excited in $TE^y_{1\delta1}$ mode. In addition, the gain of the antenna has improved from 5.04 dBi to 9.76 dBi. This encouraging result is a promising sign for the use of higher-order mode, $TE^y_{1\delta3}$ in the 5G applications.

References

[1] Rappaport TS, Sun S, et al. Millimeter Wave Mobile Communications for 5G Cellular: It Will Work!. *IEEE Access.* 2013; 1: 335-349.

[2] Boccardi F, Heath RW, Lozano A, Marzetta TL, Popovski. P, Five Disruptive Technology Directions for 5G. *IEEE Commmunication Magazine.* 2014; 52(2): 74-80.

[3] Nor NM, Jamaluddin MH, Kamarudin MR, Khalily M. Rectangular Dielectric Resonator Antenna for 28 GHz Applications. *Progress in Electromagnetics Research C.* 2016; 63: 53-61.

[4] Petosa A. Dielectric Resonator Antenna Handbook. Noorwood, MA: Artech House. 2007.

[5] Luk KM, Leung KW. Dielectric Resonator Antenna. England: Research Studies Press. 2002.

[6] Nannini C, Ribero JM, Dauvignac JY, Pichot C. Bifrequency Behaviour and Bandwidth Enhancement of a Dielectric Resonator Antenna. *Microw. Opt. Technol. Lett.* 2004; 42(5): 432-434.

[7] Nasmuddin, Esselle K. *Antennas with Dielectric Resonators and Surface Mounted Short Horns for High Gain and Large Bandwidth*. IET Proc. Microw. Antennas Propag. 2007; 1(3): 723-728.

[8] Carrie J, et al. *A. K-Band Circularly Polarized Cavity Backed Dielectric Resonator.* IEEE Antennas and Propagation Symp. Digest AP-S. Baltimore, MD, USA. 1996: 734-737.

[9] Antar YMM. *Antennas for wireless communications: Recent advances using dielectric resonators*. IET Proc. Circuits, Devices Syst. 2008; 2(1): 133-138.

[10] Petosa A, Thirakoune S. Rectangular Dilectric Resonator Antennas with Enhanced Gain. *IEEE Trans. Antennas Propag.* 2011; 59(4): 1385-1389.

[11] Antar YMM, Fan Z. *Theoretical Investigation of Aperture-Coupled Rectangular Dielectric Resonator Antenna*. IEE Proc.-Microwave Antennas Propag. 1996; 143(2): 113-118.